

Vortex dynamics in two-dimensional Josephson junction arrays

Md. Ashrafuzzaman,¹ Massimiliano Capezzali,^{1,2} and Hans Beck¹¹*Institut de Physique, Université de Neuchâtel, Rue A.L. Breguet, 2000 Neuchâtel, Switzerland*²*Cellular Biophysics and Biomechanics Laboratory, EPFL, 1015 Lausanne, Switzerland*

(Received 2 June 2003; published 7 August 2003)

The dynamic response of two-dimensional Josephson junction arrays close to, but above the Berezinskii-Kosterlitz-Thouless (BKT) transition temperature is described in terms of the vortex dielectric function $\epsilon(\omega)$ and the flux noise spectrum $S_\phi(\omega)$. They are calculated by considering both the contributions of free vortices interacting through a screened Coulomb potential and the pair motion of vortices that are closer to each other than the BKT correlation length. This procedure allows us to understand various anomalous features in $\epsilon(\omega)$ and in $S_\phi(\omega)$ that have been observed both experimentally and in dynamic simulations.

DOI: 10.1103/PhysRevB.68.052502

PACS number(s): 74.50.+r, 74.25.Qt

Neglecting capacitive effects, two-dimensional (2D) Josephson junction arrays (JJA's) are described by the classical XY model in which the superconducting phases θ_l of neighboring sites l are coupled by the Josephson interaction. The relevant excitations are vortices and antivortices, which behave as a 2D neutral Coulomb gas (CG).¹ Their charge q_0 is linked to the Josephson coupling J by $q_0^2 = 2\pi J$. At the Berezinskii-Kosterlitz-Thouless (BKT) transition the CG crosses over from a dielectric phase consisting of vortex-antivortex pairs to a metallic phase containing free vortices and antivortices. The main signature is the universal jump of the helicity modulus at T_{BKT} . It has been observed experimentally in the current-voltage characteristics of the JJA and in its response to a low-frequency electromagnetic field.^{1,2}

The dynamic behavior of JJA's is less well understood. For the equations of motion of the superconducting phases, the resistively shunted junction model can be used. Based on it, an equation of motion for the vortex excitations was derived³; it describes them as massless point particles, subject to a friction force stemming from normal current losses and interacting via the 2D Coulomb interaction, which essentially varies logarithmically with their distance. The dynamic response is described by the dielectric function $\epsilon(\omega)$. A simple approximation above T_{BKT} is given by Drude's form. Minnhagen⁴ developed a more sophisticated expression for $\epsilon(\omega)$ assuming it can be derived from the static wave-number-dependent dielectric function, taken to have a Debye screening form, replacing wave number by frequency. The result—usually referred to as “Minnhagen phenomenology” (MP)—substantially differs from Drude's (D) behavior. In particular $\text{Re}[1/\epsilon_D(\omega)] \propto \omega^2$, whereas $\text{Re}[1/\epsilon_{MP}(\omega)] \propto |\omega|$, while the so-called “peak ratio” $r = \text{Im}[1/\epsilon(\omega_m)]/\text{Re}[1/\epsilon(\omega_m)]$, ω_m being the frequency at which $\text{Im}[1/\epsilon(\omega)]$ is maximal, is $r_D = 1$, whereas $r_{MP} = 2/\pi$. Vortex dynamics below T_{BKT} is usually treated by averaging the dynamic polarizability of a pair of size d over a probability distribution for d .^{5,6}

Three main types of experiments aim at elucidating dynamical properties of JJA's. First, the exponent of the nonlinear current-voltage characteristics is related to the dynamic critical exponent describing the critical slowing down of the two-dimensional CG near the BKT transition.¹ Second, the dynamic conductance $G(\omega)$ of the array can be

inferred from measuring the dynamic response of the array to a time-dependent current in a two-coil experiment.^{1,2,7} Measurements on arrays in an external magnetic field⁸ have produced results that are closer to MP than to Drude's prediction, as far as the peak ratio and frequency dependence of $1/\epsilon(\omega)$ are concerned: $\text{Re}[1/\epsilon(\omega)] \propto |\omega|$ over a sizable range of frequencies. Third, measuring the temporal fluctuations of the magnetic flux through a given area of a JJA (Refs. 9 and 10) also provides insight into the dynamics of the currents in the array and, thus, of the vortex system. At sufficiently low frequencies, above T_{BKT} , the time Fourier transform $S_\phi(\omega)$ of the noise is white (i.e., frequency independent). At larger ω , these experiments unexpectedly show a rather extended region where $S_\phi(\omega) \propto \omega^{-1}$, which needs a deeper explanation.

Aiming at explaining the anomalous dynamics of JJA's, as revealed by the above-mentioned experiments, analytical calculations^{6,11,12} as well as dynamic simulations for JJA's have been performed based on the equations of motion for the phases of the array^{13–16} or for the CG.¹⁷ In particular, the extensive numerical efforts of Minnhagen and collaborators confirmed the existence of a frequency interval in which an anomalous MP dynamics emerges, both for zero and finite magnetic fields; analytical calculations have also been able to reproduce some characteristic features of the anomalous MP vortex dynamics upon invoking screening effects and dynamical scaling arguments.¹⁶ However, the flux noise spectra obtained within MP framework usually only show a common $1/\omega$ tangent to the curves for different temperatures, but no extended region with $1/\omega$ noise. For higher frequencies $S_\phi(\omega) \propto \omega^{-3/2}$,^{18–20} which is characteristic of vortex diffusion or $S_\phi(\omega) \propto \omega^{-2}$, for even higher frequencies.²⁰ Other calculations do yield $1/\omega$ noise²¹ or $S_\phi(\omega) \propto \omega^{-a(T)}$ with an exponent $a(T)$ close to unity, but slowly varying with temperature.¹³

The analytical approach to JJA dynamics proposed here is based on the overdamped equations of motion for the 2D neutral CG, containing a friction and an interaction term. The observables of interest are related to dynamic correlation function of hydrodynamic variables, such as

$$\phi_{\rho\rho}(\mathbf{k}, \omega) = \int_0^\infty dt e^{i\omega t} \langle \rho(\mathbf{k}, t) \rho^*(\mathbf{k}) \rangle, \quad (1)$$

where $\rho(\mathbf{k}) = 1/\sqrt{N} \sum_l q_l e^{i\mathbf{k} \cdot \mathbf{R}_l}$ is the Fourier transform of the charge density ($q_l = \pm 1$). The equal time correlator $S(k) = \langle |\rho(\mathbf{k})|^2 \rangle$ is the CG charge structure factor. From $\phi_{\rho\rho}(\mathbf{k}, \omega)$ one gets the dynamic charge susceptibility and the dielectric function of the CG,²² which may be expressed in terms of dynamic vortex mobility $\mu(\omega)$:

$$\epsilon(\omega) = 1 - 2i\pi q_0^2 \mu(\omega) \omega^{-1}. \quad (2)$$

Assuming that supercurrent is the main source of the flux threading through a coil of radius R , at a distance d from the array plane, $S_\phi(\omega)$ is related to $\phi_{\rho\rho}(\mathbf{k}, \omega)$ (Ref. 16):

$$S_\phi(\omega) = S_0 \int_0^\infty dk \frac{J_1(kR)^2 e^{-2kd}}{k(1+\lambda k)^2} \text{Re}[\phi_{\rho\rho}(k, \omega)]. \quad (3)$$

$J_1(x)$ is the first-order Bessel function and λ represents the magnetic penetration depth of the JJA.

Treating vortex dynamics above T_{BKT} analytically represents a tough challenge, since the presence of both free particles and bound pairs, predicted by the *static* scaling analysis of the BKT problem, should be taken into account. As is customary in treating the dynamics of Coulomb systems,²³ we introduce a screened effective two-body potential $V_{sc}(r)$; the latter is determined by the basic length scale of the problem: namely, the BKT correlation length $\xi(T)$. At distances $r < \xi(T)$, $V_{sc}(r)$ exhibits *dielectric* screening via a length-dependent dielectric function $\epsilon(r)$, obtained through static BKT scaling: $V_{sc}^d(r) = q_0^2 \epsilon(r)^{-1} \ln(r/a)$. Conversely, at $r > \xi(T)$, $V_{sc}(r)$ incorporates *metallic* Debye screening, given by $V_{sc}^m(k) = q_0^2 / (k^2 + \xi^{-2})$ in reciprocal space. As our hydrodynamic variables are typically sums of single-particle terms, dynamic correlators, such as Eq. (1), are evaluated by correlating the trajectory $R_l(t)$ of a given particle with the initial position $R_l(0)$ of another one. In such a trajectory, one can distinguish essentially two different types of motion, each being realized over some time span: when a particle has found a partner of opposite charge closer than $\xi(T)$, the two will temporarily form a pair interacting through $V_{sc}^d(r)$. Their contribution to a given dynamic correlation function will look like the one of a single pair, as has been treated by Ambegaokar *et al.*,⁵ including, however, a finite lifetime. On the other hand, when our particle does not own a partner for temporary pairing within the distance $\xi(T)$, it will essentially behave like a free—i.e., unbound—particle, moving under the influence of $V_{sc}^m(r)$, and the corresponding contribution to a given correlation function will be calculated taking into account only the metallicly screened potential. The detailed techniques we have used for evaluating both contributions are described below.

An analytical approach does not permit one to follow each trajectory $R_l(t)$ in order to distinguish these two types of time evolution. In order to account, in an average sense, for paired and free motion, we use the fact that our dynamic correlation functions are given by a statistical average over a canonical ensemble of initial configurations. Such an equilibrium configuration, at a given temperature, is characterized by the BKT correlation length: charges of opposite sign which are closer to each other than $\xi(T)$ are supposed to be

bound in pairs whereas all the remaining ones are free. As usual in the treatment of the BKT problem, more complicated configurations, such as double pairs, are neglected, which is appropriate for low densities of particles. We introduce the average fractions $\nu_f \propto \xi^{-2}$ and $\nu_b = 1 - \nu_f$ of free and paired particles, respectively, out of a total of n particles in thermal equilibrium and then calculate the reaction of the whole system by adding the contribution of the pairs and of the free particles to some response function with these weights. This strategy is built on the assumption that the main pair correlations entering correlators like $\phi_{\rho\rho}(\mathbf{k}, \omega)$ are those which result from the initial paired (free) configurations, whereas pair (free) motion that occurs at later times will be included in an average (time independent) way through the distance-dependent screened Coulomb interaction.

We consider the vortex mobility $\mu(\omega)$ as the central response function for which we will combine the respective contributions of pair and free motion. $\mu(\omega)$ directly determines $\epsilon(\omega)$, via Eq. (2) as well as $\phi_{\rho\rho}(\mathbf{k}, \omega)$.¹⁶ The total mobility of the vortex system above T_{BKT} shall thus be approximated by a superposition of pair and free contributions: $\mu(\omega) = (1 - \nu_f)\mu_b(\omega) + \nu_f\mu_f(\omega)$, in analogy to electric circuits put in parallel. According to Eq. (2), a corresponding superposition will hold for the dielectric function. Adding bound and free contributions to $\epsilon(\omega)$ also results from a rigorous T -matrix analysis of the dynamics of quantum Coulomb gas.²⁴ Hereafter, we delineate the methods used to derive $\mu_f(\omega)$ and $\mu_b(\omega)$.

(a) The *free vortex* mobility $\mu_f(\omega)$ is determined by using Mori's technique of calculating dynamic correlation functions to $\phi_{\rho\rho}(\mathbf{k}, \omega)$.^{6,12} As usual, higher-order correlators—arising upon using the equations of motion for the individual particles—are factorized. This should be adequate as we use the screened interaction between two given particles, which incorporates correlations with other particles in an average sense. In Mori's approach, the inverse of the mobility—i.e., the vortex friction function—is given by the force-force correlation function (for details, see Refs. 6 and 12). The resulting density correlator (1) is

$$\phi_{\rho\rho}(\mathbf{k}, \omega) = \frac{S(\mathbf{k})}{-i\omega + \frac{k_B T k^2 \mu(\omega)}{S(\mathbf{k})}}. \quad (4)$$

We choose a Debye-Hückel form $S(k) = k^2 / (k^2 + k_0^2)$,²² with $k_0^2 = 2\pi q_0^2 n / k_B T$ and n being the total vortex density—which respects both the charge neutrality of the vortex system and the correct limit for large k ; thereby, both diffusion and relaxation dynamics—typically arising in a Coulomb system—clearly appear in Eq. (4). Three frequency regimes emerge, separated by the scale frequencies $\omega_a = k_B T / \Gamma a^2$ (a is the lattice constant) and $\omega_\xi = k_B T / \Gamma \xi^2$. Here $\text{Re}[\mu_f(\omega)^{-1}]$ is flat for $\omega < \omega_\xi$ with a value increasing as ξ^2 —it coincides with the bare friction parameter Γ for $\omega > \omega_a$ —whereas $\text{Re}[\mu_f(\omega)^{-1}] \propto \ln|\omega|$ in between.^{11,12} The resulting inverse dielectric function, shown in Fig. 1, indeed follows MP behavior— $\text{Re}[\epsilon(\omega)^{-1}] \propto \omega$ for $\omega_\xi < \omega < \omega_a$ —for a fre-

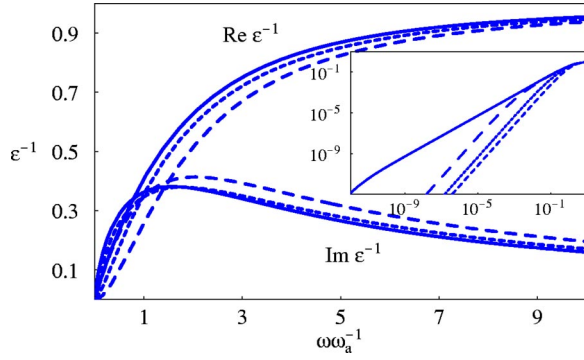


FIG. 1. $\text{Re}[1/\epsilon(\omega)]$ and $\text{Im}[1/\epsilon(\omega)]$ vs ω/ω_a for free dynamics. Solid, short-dashed, and long-dashed lines are for $t=T/T_{BKT} = 1.01, 1.10,$ and 1.20 . The inset represents the log-log plot for $\text{Re}[1/\epsilon(\omega)]$ with $t=1.05$ (dashed line) in addition to the other three temperatures.

frequency range that increases when T_{BKT} is approached. Moreover, the values of the peak ratio vary between 0.67 and 0.73 for the three temperatures shown in Fig. 1, closer to MP than to Drude behavior. Thus, insofar as the contribution of free vortices is concerned, anomalous MP dynamics is explained by the increasing influence of the long-range Coulomb force, which makes motion more and more *sluggish*. Whereas at high temperatures the potential is (metallically) screened for all relevant length scales, screening becomes less and less efficient on approaching T_{BKT} , where the screening length ξ diverges. However, contrary to MP, we obtain a response which always crosses over to Drude like when $\omega < \omega_\xi$; if this were not the case, the array would still be superconducting above T_{BKT} ,¹⁰ whereas in reality a finite flux-flow resistance yields a finite conductance at zero frequency. The flux noise spectrum we obtain considering only free vortices, however, does not show any extended $1/\omega$ region. Notably enough, both resulting $1/\epsilon(\omega)$ and $S_\phi(\omega)$ compare satisfactorily with Minnhagen and co-workers' simulations.^{14,17} One may thus draw the conclusion that anomalous MP behavior for the dielectric function does not yield the—equally anomalous— $1/\omega$ noise, which should thus have a different origin.

(b) For the *paired vortex* mobility $\mu_b(\omega)$, following Ref. 5, we average the dynamic polarizability of a single pair over a suitable probability distribution function $\phi(r)$ for the pair size r (Refs. 5 and 6):

$$\chi(z) = \int_a^\infty r dr \frac{\phi(r)}{z\Gamma + f(r) + 1/\tau(r)}. \quad (5)$$

The Boltzmann factor $\phi(r) \propto e^{-\beta q_0^2 \ln(r/a)/\epsilon(r)} \theta(\xi - r)$ is cut off at the BKT correlation length, where the scaled potential ceases to be attractive. The force constant in the denominator of Eq. (5) is given by $f(r) = q_0^2/r^2 \epsilon(r)$, and we have also introduced a finite pair lifetime⁶ $1/\tau(r) = \omega_0 \exp\{q_0^2 \ln(\xi/a)/\epsilon(d_c) - q_0^2 \ln(r/a)/\epsilon(r)\}$ where ω_0 is a free parameter representing an attempt frequency for pairs trying to escape the barrier up to the maximum of the potential, at the distance ξ , by thermal excitation. From the polarizability

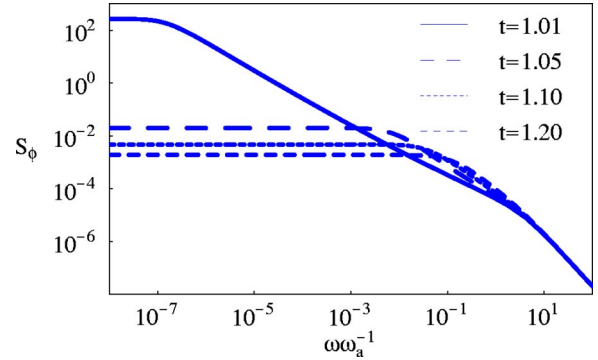


FIG. 2. $S_\phi(\omega)$ vs ω/ω_a for pair dynamics with $k_0^2 = 2\pi q_0^2 n/k_B T$ and $t=T/T_{BKT}$.

(5), by the usual relations for Coulomb systems,²³ one obtains the corresponding pair mobility $\mu_b(\omega)$, the corresponding charge correlator (4) and the pair dielectric function $\epsilon_b(\omega)$. Three frequency regimes can be distinguished. (i) Drude behavior $\text{Re}[1/\epsilon_b(\omega)] \propto \omega^2$ extends up to a critical frequency $\omega_c \sim \xi^{-2}$. (ii) In the window $\omega_c < \omega < \omega_a$, $\text{Re}[1/\epsilon_b(\omega)] \propto \omega^{s(T)}$, where the T -dependent exponent $s(T) \approx 1/3$ near T_{BKT} and decreases with increasing T ; its value is determined by the detailed r dependence of ϕ , f , and $1/\tau$ in the integral equation (5). (iii) Finally, for $\omega > \omega_a$, the high-frequency Drude form is recovered. The flux noise resulting from paired motion is shown in Figs. 2 and 3. Choosing $k_0^2 = k_B T/2\pi q_0^2 n$, n being taken from Ref. 14—i.e., a length proportional to the mean distance between particles—yields $S_\phi(\omega) \propto \omega^{-a(T)}$, with $a(T) = 1$ at T_{BKT} and increasing above (Fig. 2). We notice that the curves for different temperatures cross each other (there is a hint that this also happens in the experimental data of Ref. 10). On the other hand, having taken into account only the response of single pairs, it seems more appropriate using the mean structure factor for an ensemble of independent pairs; then, $k_0^2 = \pi^2/\langle r^2 \rangle$, where $\langle r^2 \rangle$ is the T -dependent mean square of the pair size calculated using Boltzmann factor $\phi(r)$. The resulting flux noise spectrum (Fig. 3) varies as $1/\omega$ and all the curves for different temperatures fall on top of each other for $\omega > \omega_c$, as is seen in the experiments.^{9,10} The white noise level showing up for $\omega < \omega_c$ is also strongly T dependent and is given by $S_\phi(0) \propto [\mu_b(0)^{-1}/k_B T n](k_B T/J)^2$.

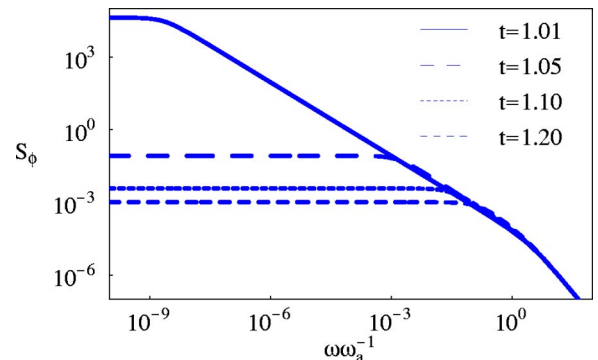


FIG. 3. $S_\phi(\omega)$ vs ω/ω_a with T -dependent $k_0^2 = \pi^2/\langle r^2 \rangle$ for pair dynamics and $t=T/T_{BKT}$.

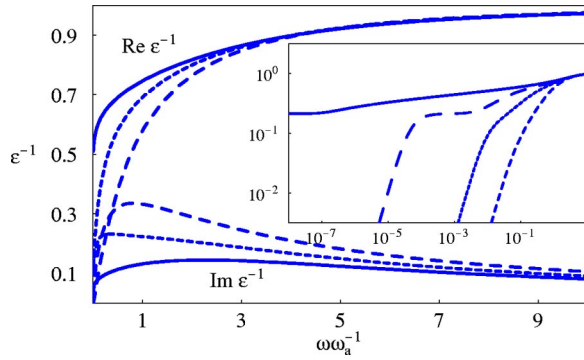


FIG. 4. $\text{Re}[1/\epsilon(\omega)]$ and $\text{Im}[1/\epsilon(\omega)]$ vs ω/ω_a using the combined mobility pair and free dynamics. Solid, short-dashed, and long-dashed lines are for $t=T/T_{BKT}=1.01, 1.10, \text{ and } 1.20$. The inset represents the log-log plot for $\text{Re}[1/\epsilon(\omega)]$ with $t=1.05$ (dashed line) in addition to the other three temperatures.

The critical contribution comes from $\mu_b(0) \sim \xi^{-2}$ and thus $S_\phi(0) \sim \xi^2$. However, when ξ reaches the sample size, $\mu_b(0)$ saturates and the T dependence of $S_\phi(0)$ is dominated by the total density n of vortex excitations. This “masking” of the true critical slowing down has been observed in Ref. 10.

As a final step we combine the two contributions to obtain

the total mobility $\mu(\omega)$. The contribution of pairs is still dominant up to $T/T_{BKT}=1.1$, since its weight is larger, although the free vortices mobility itself exceeds the one of bound pairs. Combining the two contributions (Fig. 4) yields a rather extended flat region of $\text{Im}[1/\epsilon(\omega)]$ for intermediate frequencies, which is another signature of anomalous vortex dynamics, also emerging from numerical simulations.¹⁴

In conclusion, our analytical calculations, combining *free* and *pair* motion, give the following insight into vortex dynamics in JJA's above the BKT temperature: (i) The anomalous Minnhagen phenomenology is a consequence of the motion of (unbound) vortices in a Coulomb potential which is screened by other *free* particles. The more this screening decreases upon approaching transition temperature, the more anomalous behavior is pronounced. However, MP does not lead to $1/\omega$ flux noise. (ii) Vortices and antivortices moving as *pairs*, at short enough distances and up to some finite lifetime, yield an even more anomalous vortex dielectric constant with temperature-dependent frequency exponents. This effect, combined with a T -dependent pair structure factor indeed gives $1/\omega$ flux noise in an intermediate-frequency range.

We thank P. Martinoli, D. Bormann, and S. Korshunov for interesting discussions. This work was supported by the Swiss National Science Foundation.

- ¹For a summary of experimental work see, e.g., R.S. Newrock, C.J. Lobb, U. Geigenmüller, and M. Octavio, *Solid State Phys.* **54**, 263 (2000).
- ²P. Martinoli and Ch. Leemann, *J. Low Temp. Phys.* **118**, 699 (2000).
- ³H. Beck and D. Ariosa, *Solid State Commun.* **80**, 657 (1991).
- ⁴P. Minnhagen, *Rev. Mod. Phys.* **59**, 1001 (1987).
- ⁵V. Ambegaokar, B.I. Halperin, D.R. Nelson, and E.D. Siggia, *Phys. Rev. Lett.* **40**, 783 (1978); *Phys. Rev. B* **21**, 1806 (1980).
- ⁶D. Bormann, H. Beck, O. Gallus, and M. Capezzali, *J. Phys. IV* **10**, Pr5-447 (2000).
- ⁷P. Martinoli, Ph. Lerch, Ch. Leemann, and H. Beck, *Jpn. J. Appl. Phys., Part 1* **26-3**, 1999 (1987).
- ⁸R. Théron, J.B. Simond, Ch. Leemann, H. Beck, P. Martinoli, and P. Minnhagen, *Phys. Rev. Lett.* **71**, 1246 (1993).
- ⁹T.J. Shaw, M.J. Ferrari, L.L. Sohn, D.H. Lee, M. Tinkham, and J. Clarke, *Phys. Rev. Lett.* **76**, 2551 (1996).
- ¹⁰S. Candia, Ch. Leemann, S. Mouaziz, and P. Martinoli, *Physica C* **369**, 309 (2002).
- ¹¹S.E. Korshunov, *Phys. Rev. B* **50**, 13 616 (1994); H. Beck, *ibid.* **49**, 6153 (1994).
- ¹²M. Capezzali, H. Beck, and S.R. Shenoy, *Phys. Rev. Lett.* **78**, 523 (1997).
- ¹³P.H.E. Tiesinga, T.J. Hagenaars, J.E. van Himbergen, and J.V. Jose, *Phys. Rev. Lett.* **78**, 519 (1997).
- ¹⁴A. Jonsson and P. Minnhagen, *Phys. Rev. B* **55**, 9035 (1997); K. Medvedyeva, B.J. Kim, and P. Minnhagen, *Physica C* **355**, 6 (2001).
- ¹⁵L.M. Jensen, B.J. Kim, and P. Minnhagen, *Phys. Rev. B* **61**, 15 412 (2000) and references therein.
- ¹⁶Md. Ashrafuzzaman and H. Beck, *Studies of High Temperature Superconductors* (Nova Science, New York, 2002), Vol. 43.
- ¹⁷B.J. Kim and P. Minnhagen, *Phys. Rev. B* **63**, 094514 (2001).
- ¹⁸Carsten Timm, *Phys. Rev. B* **55**, 3241 (1997).
- ¹⁹I. Hwang and D. Stroud, *Phys. Rev. B* **57**, 6036 (1998).
- ²⁰B.J. Kim and P. Minnhagen, *Phys. Rev. B* **60**, 6834 (1999).
- ²¹K.H. Wagenblast and R. Fazio, *JETP Lett.* **68**, 312 (1998).
- ²²N.H. March and M.P. Tosi, *Atomic Dynamics in Liquids* (Wiley, New York, 1976), Chap. 9.
- ²³H.E. DeWitt, M. Schlanges, A.Y. Sakakura, and W.D. Kraeft, *Phys. Lett. A* **197**, 326 (1995).
- ²⁴G. Röpke and R. Der, *Phys. Status Solidi B* **92**, 501 (1979).